PROTEINS: Structure, Function, and Genetics 37:310–318 (1999)

Role of Metal Ions on the Secondary and Quaternary Structure of Alkaline Phosphatase From Bovine Intestinal Mucosa

Muriel Bortolato,* Françoise Besson, and Bernard Roux
Laboratoire de Physico-Chimie Biologique, Université Claude Bernard Lyon I, Villeurbanne, Cedex, France

ABSTRACT **Alkaline phosphatase (EC 3.1.3.1) from bovine intestinal mucosa (BIAP) is an homodimeric metalloenzyme, containing one Mg^{2+} and two Zn^{2+} ions in each active site. ApoBIAP, prepared using ion-chelating agents, exhibited a dramatic decrease of its hydrolase activity, concomittant to conformational changes in its quaternary structure. By rate-zonal centrifugation and electrophoresis, we demonstrated, for the first time, that the loss of divalent ions leads to some monomerization process for a metal-depleted alkaline phosphatase. Divalent ions are also involved in the secondary and tertiary structures. Metal-depletion induced more exposure of some Trp residues and hydrophobic regions to the solvent (as proved by intrinsic and ANS fluorescences). These changes might correspond to the disappearance of α-helices and/or turns with a concomittant appearance of unordered structures and β-sheets (as probed by FTIR spectroscopy). For BIAP, three steps of temperature-induced changes were exhibited, while for apoBIAP, only one step was exhibited at 55°C. Our work on BIAP showed two main differences with alkaline phosphatase from *Escherichia coli.* The loss of the divalent ions induces protein monomerization and the total recovery of enzyme activity by divalent ion addition to apoBIAP was not obtained. Proteins 1999;37:310–318.** © 1999 Wiley-Liss, Inc.

Key words: FTIR; metalloenzyme; apoenzyme

INTRODUCTION

Divalent metal ions serve to enhance the structural stability of a protein in a conformation that is critical for its biological function or take part in the catalytic processes of enzymes. Therefore, it is interesting to study the influence of metals on the conformation of a metalloenzyme, the alkaline phosphatase from bovine intestinal mucosa.

Alkaline phosphatase is a widely distributed enzyme and it has been isolated from eukaryotes as well as from procaryotes. It hydrolyzes non-specifically phosphate monoesters at alkaline pH to produce inorganic phosphate and an alcohol.[1] Intensive studies have been done on ECAP (for review, see Coleman[2]). The active site of this phosphatase has been well characterized by site-directed mutagenesis,[3–12] by X-ray crystallography on the wild-type[13,14] and on several mutants,[15–23] and by NMR.[1,24] On the basis of these studies it is now accepted that AP is an homodimeric enzyme containing in each active site (one per monomer and 30Å apart) one phosphorylatable serine and three distinct metal binding sites for one magnesium and two zinc ions. Active site is located in a pocket created by the termination of a number of helices and sheets that is open to the surface.[14] Previous studies on ECAP have shown the importance of the divalent metal ions: magnesium does not directly participate in the mechanism but is important for structural stabilization of the enzyme, whereas the two zinc ions are directly involved in catalysis.[25,26] The two zinc ions are well positioned to activate the serine and water for nucleophilic attacks and they are involved in holding of the phosphate portion of substrate.[14] One zinc ion is required for catalysis and plays an important role in binding both the substrate and phosphate. The second one interacts with the hydroxyl group of the active serine to stabilize the deprotonated form of serine necessary for the nucleophilic attack on the phosphate. The main amino acid residues that serve as ligands to divalent ions are Asp, His, Thr, and Glu.[13,14]

Mammalian APs are glycoproteins that are present as different isoenzymes in several tissues including bone, intestine, kidney, and placenta. Very little is known about structure of mammalian APs. They are zinc-metalloenzymes which can be activated by magnesium ions; both ions are essential for catalysis and stability.[27–33] Based on the refined structure of ECAP[13] and the sequences of mammalian enzymes, Kim and Wyckoff[34] have modelled the core of the three-dimensional structures of the mammalian APs. The active-site region is highly conserved but specific changes in the secondary ligands to bound phosphate and the Mg^{2+} ions are observed.

Like all the mammalian APs,[35] bovine intestinal mucosa enzyme is anchored in the membrane. The sequence of the protein has limited homology (26%) with those of *Esch-*

Abbreviations: ANS, (1-anilino-8-naphtalenesulfonate); AP, alkaline phosphatase; BIAP, alkaline phosphatase from bovine intestinal mucosa; apoBIAP, metal-depleted BIAP; ECAP, alkaline phosphatase from *Escherichia coli*; FTIR, Fourier transform infrared spectroscopy.

Grant sponsor: the Centre National de la Recherche Scientifique UPRESA-CNRS 5013.

*Correspondence to: Muriel Bortolato, Laboratoire de Physico-Chimie Biologique UPRESA-CNRS 5013, Université Claude Bernard Lyon I, 43, bd du 11 novembre 1918, F-69622 Villeurbanne, Cedex, France. E-mail: bortolat@univ-lyon1.fr

Received 16 March 1999; Accepted 21 May 1999

erichia coli, except for the 10 residues immediately flanking the active-site serine (70%).[36]

Preliminary studies on BIAP showed that thermal or acidic pH inactivations of the enzyme activity occurred at lower temperature and higher pH than the conformational changes observed by FTIR spectroscopy.[37] In the present work, the influence of divalent ions on the enzymatically active structure of BIAP was studied by using centrifugation analysis and different spectroscopic methods.

MATERIALS AND METHODS

Materials

Deuterium oxide (^2H_2O), at 99.9% isotopic purity, was obtained from Merck (Darmstadt, Germany). Pyridine-2,6-dicarboxylic acid (or dipicolinic acid), ANS and soluble BIAP type VII-NL were purchased from Sigma. Enzyme purity was verified by gel electophoresis. Econo-Pac 10DG column was obtained from Bio-Rad. The salts used in buffer preparation were of analytical grade.

Enzyme and Apoenzyme Preparation

Commercial BIAP powder contains Tris-citrate buffer that was removed by dialysis. Its elimination was verified by infrared spectroscopy. Samples were then lyophilized and resuspended in the suitable solution. This procedure does not alter the enzyme intrinsic metal content as shown by the Zn^{2+} and Mg^{2+} determination. Apoenzyme was prepared by dialysis against 150 mM Tris-HCl pH 7.5 buffer containing 20 mM of dipicolinic acid, as metal chelator. The apoBIAP, after separation from the chelator-metal complex by passing the mixture trough an EDTA-washed DG-10 column, was lyophilized and resuspended in deionized water or metal-free buffer prepared according to the method of Holmquist.[38] The absence of dipicolinic acid in protein samples was verified by infrared spectroscopy.

Zn and Mg Content Determination

Plasma emission spectroscopy or ICP-MS (Service Central d'Analyse, CNRS, Vernaison, France) was used to determine Zn^{2+} and Mg^{2+} content in enzyme and apoenzyme.

Enzyme Activity

Enzyme aliquots were diluted in 10 mM glycine-NaOH pH 10.4 buffer containing the enzyme substrate *p*-nitrophenyl phosphate. Activities were measured spectrophotometrically at 37°C by monitoring the release of *p*-nitrophenolate at 420 nm (ϵ = 18.5 cm^2/µmol). One unit of specific activity hydrolyses 1 µmol of substrate per min per mg of protein (U/mg).

Analytical Rate-Zonal Centrifugation

Analytical centrifugation was performed on 5–20% (w/w) sucrose isokinetic gradients in Tris-HCl 10 mM pH 7.4 buffer. 200 µg of analyzed protein were suspended in Tris-HCl 10 mM pH 7.4, SDS 0.2% buffer and were layered individually on gradients. Centrifugation was carried out in an SW 40 Ti rotor for 20 h at 5°C and 36,500 rpm in a Beckman L5–50B ultracentrifuge. Approximately 65 fractions of 200 µL were collected and assayed for enzymatic activity. Protein content was monitored by the fluorescence emission at 330 nm (excitation 290 nm) with a SFM 23 KONTRON fluorescence spectrometer.

Analytical Electrophoresis

Electrophoresis was performed in 15.2% (w/v) polyacrylamide gels, according to the method of Ryrie and Gallagher[39] modified from Laemmli,[40] under non-denaturating conditions (samples were prepared in 0.1% SDS without heating before migration). Proteins were stained with Coomassie Brilliant Blue R.

Infrared Spectroscopy

Solutions of BIAP and apoBIAP (10 mg/mL) were freshly prepared in ^2H_2O. FTIR spectra were recorded by means of a Nicolet 510 M FTIR spectrometer (DTGS detector) using a temperature-controlled flow-through (model TFC-M25; Harrick Scientific Corp., Ossining, NY) equipped with 50 µm spacers and CaF_2 windows. Typically 128 scans at 4 cm^{-1} resolution were taken, coadded and Fourier transformed. During data acquisition, the spectrometer was continuously purged with dry air filtered with a Balston regenerating desiccant dryer (model 75–45 12 VDC). The infrared spectrum of buffer was deduced from the sample infrared spectrum taken under the same conditions. For thermal denaturation, the temperature was raised from 20°C to 80°C with 5°C step. When the selected temperature was reached, it was maintained for 5 min before spectrum acquisition began.

Fluorescence Spectroscopy

Fluorescence emission spectra were recorded on a Bio-Logic fluorescence spectrometer. Each spectrum followed from three scans average and the buffer spectrum was deduced from the sample spectrum taken in the same conditions. For thermal denaturation, temperature was maintained with a thermostatically controlled cell holder.

For measurements of intrinsic fluorescence, the excitation wavelength was set at 290 nm in order to preferentially excite the four tryptophan residues per monomer. BIAP and apoBIAP concentrations were 100 µg/mL in metal-free Tris-HCl buffer 20 mM pH 7.5. The emission spectra were recorded between 300 nm and 400 nm. To obtain fluorescence unfolding profiles, the changes in protein fluorescence were expressed as intensity-weighted average emission wavelength $\langle\lambda\rangle$[41],

$$\langle\lambda\rangle = \frac{\Sigma \lambda_i F_i}{\Sigma F_i}$$

where λ_i and F_i represent respectively the wavelengths measured and the corresponding emission intensities. In a

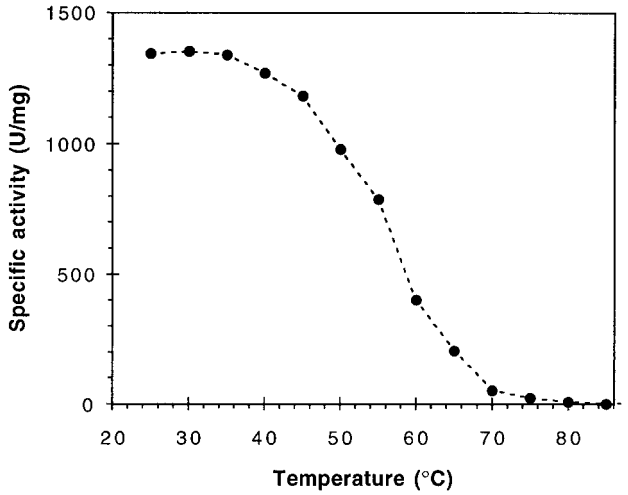

Fig. 1. Influence of temperature on the specific activity of BIAP.

two-state unfolding model, fraction unfolded for each temperature, was obtained from

$$f_u = \frac{\langle\lambda\rangle - \langle\lambda\rangle_f}{\langle\lambda\rangle_u - \langle\lambda\rangle_f}$$

where $\langle\lambda\rangle_f$ is the $\langle\lambda\rangle$ of the folded form corresponding to $\langle\lambda\rangle_{min}$ and $\langle\lambda\rangle_u$ is the $\langle\lambda\rangle$ of the unfolded form corresponding to $\langle\lambda\rangle_{max}$ (in total unfolding conditions).

For ANS assays, the excitation wavelength was set at 380 nm while the emission was recorded at 490 nm. Concentrations of ANS and proteins were respectively 19 μM and 200 μg/mL.

RESULTS

Influence of Ions and Temperature on the Specific Activities of Alkaline Phosphatase

BIAP and apoBIAP were prepared from commercial alkaline phosphatase as described in Materials and Methods. The determination of the metal content of the two enzyme forms gave about 2 Zn^{2+} and 1 Mg^{2+} ions per monomer of BIAP and about 0.05 Zn^{2+} and 0.1 Mg^{2+} per monomer of apoBIAP. Metal depletion of the enzyme resulted in a dramatic decrease of activity, indeed apoBIAP specific activity represented only 0.5% of the native protein. Attempts of apoBIAP reactivation did not induce significant recovery of enzyme activity. When divalent ions (Mg^{2+} and Zn^{2+}) were added to apoBIAP, either by directly in the enzyme solution or by dialysis, only 5% of initial BIAP activity was restored. This demonstrates the critical role of divalent ions for the enzymatic function of BIAP.

When the enzyme was heat-denatured, BIAP exhibited a transition point for its enzymatic activity at 56°C (Fig. 1), while, in the case of apoBIAP, no transition point could be determined on account of its very low specific activity.

Influence of Ions on the Sedimentation and Electrophoresis Profiles of Alkaline Phosphatase

The oligomeric forms of BIAP and apoBIAP were determined by centrifugation on isokinetic gradients. In all the cases, the different fractions obtained by centrifugation on sucrose gradients were analyzed for the protein content by fluorescence intensity determination and for the alkaline phosphatase activity (Fig. 2). BIAP gave a single peak of enzymatically active protein, located at 6 mL or 11.75% sucrose (Fig. 2A). Standard BIAP monomer, obtained by incubation of BIAP at 100°C in the presence of SDS 2%, exhibited a single peak of enzymatically inactive protein, located at 8.4 mL or 7.5% sucrose (Fig. 2B). For apoBIAP (Fig. 2C), enzymatically active and inactive protein peaks were detected respectively at 11.75% (peak I) and 8% sucrose (peak II). Peak I represented about 75% of the total protein content, as determined by surface analysis. The specific activity of peak II represented about 1.4% of the native BIAP specific activity.

Figure 3 shows the electrophoretic profiles of characteristic fractions of the different gradients. Active BIAP gave a single band at 140 kDa, corresponding to the dimeric form (Fig. 3, lane 1), while the inactive BIAP monomer gave a single band at 60 kDa (Fig. 3, lane 2). For apoBIAP, the two protein fractions detected at 11.75% and 8% sucrose corresponded respectively to the dimeric and the monomeric forms (Fig. 3, lanes 3 and 5) and the intermediate fractions (between 11.75% and 8% sucrose) contained a dimer and monomer mixture (Fig. 3, lane 4). These results demonstrate that metal ions were necessary to stabilize the quaternary structure of BIAP.

When BIAP was heat-denatured at 60°C for 10 min, a minor peak at 7.5% sucrose appeared on the centrifugation profile (data not shown), indicating that heat-denaturation also induced some monomerization. When apoBIAP was heat-denatured in the same conditions, its centrifugation profile revealed species of higher molecular weight (data not shown), proving the aggregation of thermally denatured apoBIAP.

Influence of Ions on the FTIR Spectra of Alkaline Phosphatase

Since a correspondence was established between the position of the amide band maxima in IR spectrum and the conformations of the peptide backbone,[42–44] FTIR spectroscopy is a powerful tool for the determination of the secondary structure of proteins. The ^2H_2O-subtracted FTIR spectra of BIAP and apoBIAP at 25°C, as well as their second derivative spectra, are shown in Figure 4A, B. Table I gives the tentative assignments of the various bands according to Surewicz and Mantsch[45] and Goormaghtigh et al.[46] The remaining amide II band pointed out an incomplete N-H/N-^{2}H exchange. This correspond to N-H buried in hydrophobic regions of the protein since the amide II band intensity was not modified by increasing the incubation time with ^2H_2O.

The enzyme conformational changes induced by the loss of its ions were better seen in the calculated IR difference spectrum (Fig. 4C). The positive band at 1,632 cm^{-1} might indicate the appearance of unordered structures and β-sheets in apoBIAP, while the negative bands at 1,651 and 1,664 cm^{-1} showed respectively the disappearance of α-helices and/or turns in the native enzyme. The negative band at 1,595 cm^{-1} with a shoulder at 1,577 cm^{-1} could be

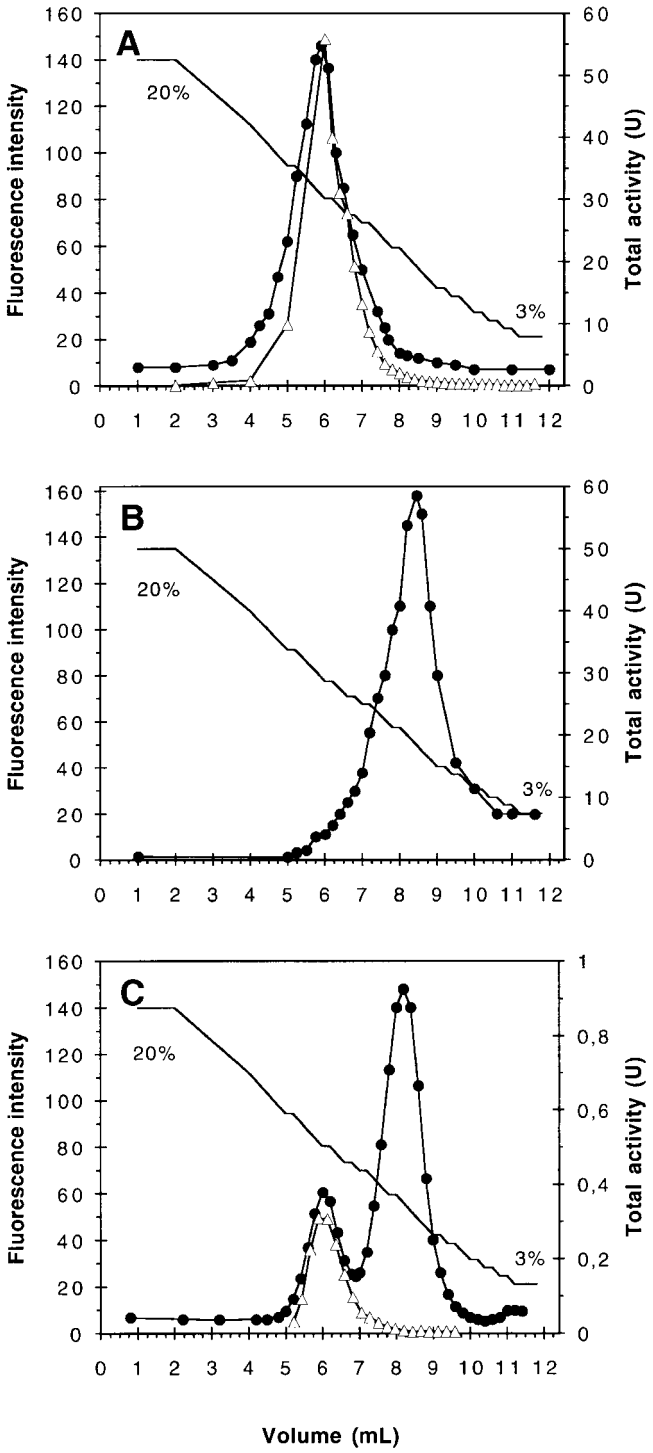

Fig. 2. Sucrose gradient centrifugation profiles of alkaline phosphatase after different treatments. **(A)**: BIAP. **(B)**: Standard BIAP monomer (incubation at 100°C in the presence of SDS 2%). **(C)**: apoBIAP. For each sample, fluorescence in arbitrary units (●), enzymatic activity (△), and sucrose percentage (—) were determined. 200 µg of each protein were layered on gradients. Fluorescence emission was measured at 330 nm with an excitation at 290 nm.

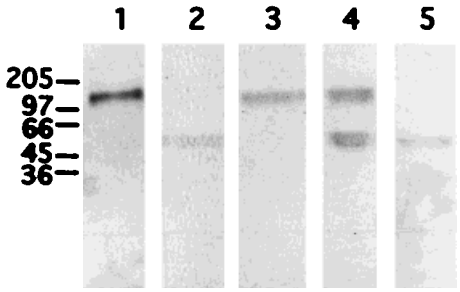

Fig. 3. Electrophoretic analysis of various fractions obtained after sucrose gradient centrifugation. **Lane 1,** fraction 11.75% sucrose of BIAP; **lane 2,** fraction 7.5% sucrose of standard BIAP monomer; **lanes 3, 4,** and **5,** respectively, fractions 11.75%, 10% and 8% sucrose of apoBIAP.

explained, at least partly, by the loss of linkage to divalent ions for the Asp and/or Glu COO^- groups of apoBIAP.[47,48] However, a contribution of more important N-H deuteration in apoBIAP cannot be excluded since there was a positive band at 1,545 cm^{-1}. Thus BIAP secondary structures are stabilized by divalent ions.

Influence of Temperature on FTIR Spectra of Native Alkaline Phosphatase and Apoenzyme

Temperature increase from 25°C to 80°C induced spectral changes for BIAP and apoBIAP which were better visualized by calculated IR difference spectra (Fig. 5). Both enzymes did not exhibit the same thermal stability. The most drastic temperature-induced changes were observed at 70–80°C for BIAP and at 55–60°C for apoBIAP and correspond to the appearance of intermolecular β-sheets (positive bands at 1,620 and 1,685 cm^{-1}) and the disappearance of some α-helices (negative band at 1,655 cm^{-1}). These conformational changes (Fig. 6) were concomittant to the deuteration of some peptide NH groups becoming accessible to ^2H_2O.[43] Moreover, in the case of BIAP (Fig. 5A), the minor temperature-induced changes at 40–50°C could be related to modifications concerning Asp and/or Glu COO^- groups (negative band at 1,570 cm^{-1})[47,48] and Arg residues (positive band at 1,610 cm^{-1})[46] near the metal binding sites. These results indicate the ion-protecting role against the thermal protein denaturation.

Influence of Temperature on Intrinsic Fluorescence of Native Alkaline Phosphatase and Apoenzyme

The position of the emission maximum of protein fluorescence upon excitation at 290 nm provides information on the exposure of Trp residues to the solvent. Figure 7A gives the fluorescence spectra of the Trp residues of BIAP and apoBIAP. The removal of divalent ions resulted in a large red-shift from 326 nm to 339 nm at 25°C which indicates higher exposure of Trp residues to solvent. The thermal denaturation of both native and apoenzyme induced a similar red-shift but the most important shift (13 nm) was observed with BIAP. Both heat-denatured forms of the enzyme did not exhibit the same maximum (339 nm for BIAP and 349 nm for apoBIAP). Thermal unfolding transition studies of BIAP and apoBIAP are shown on Figure 7B. The transition point of BIAP (about 65°C) was higher than that of the metal-depleted protein (about 50°C), indicating again the ion-protecting role against thermal denaturation of BIAP.

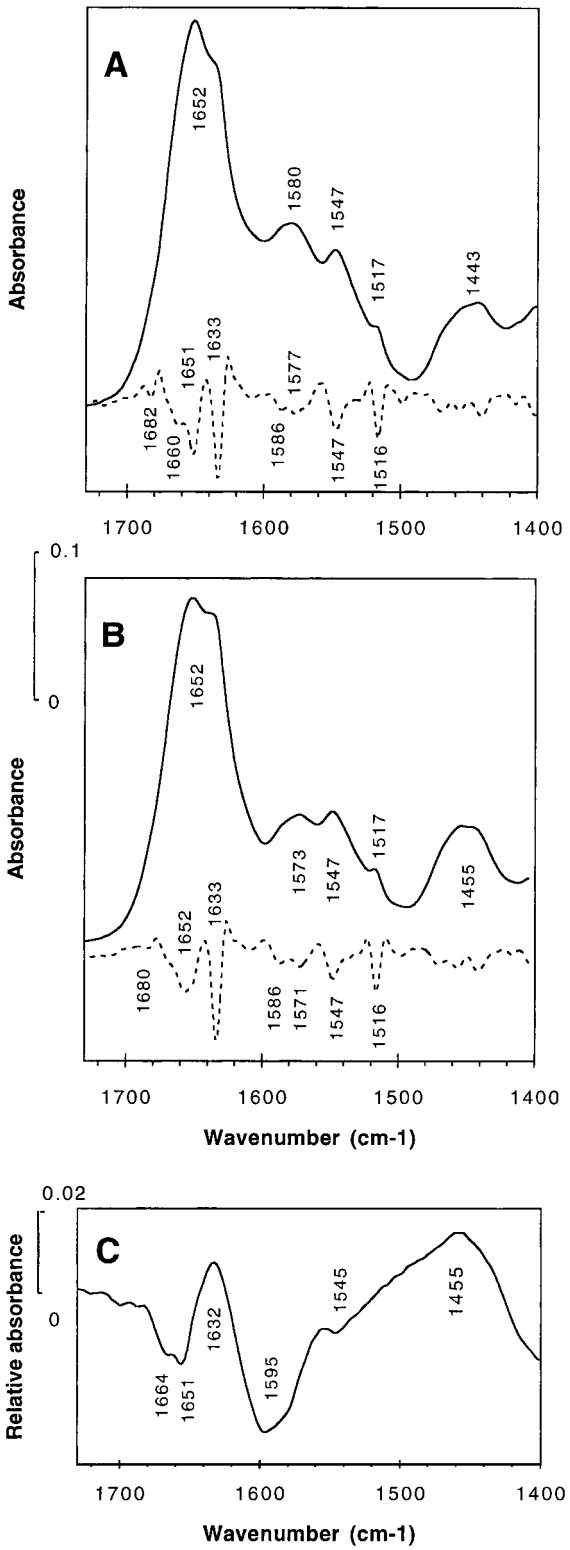

Fig. 4. Influence of divalent ions on the FTIR spectra of alkaline phosphatase in ^2H_2O pH 6.6 (10 mg/ml). **(A)**: BIAP spectra. **(B)**: apoBIAP spectra. For each protein, solvent-subtracted spectrum (—) and second derivative spectrum (---) were shown. **(C)**: IR difference spectrum calculated by subtracting BIAP FTIR spectrum (A) from apoBIAP FTIR spectrum (B).

TABLE I. Tentative Assignments of the Various Bands Observed in the Solvent-Substracted FTIR Spectra of BIAP and apoBIAP in ^2H_2O, pH 6.6

Band wavenumber (cm^{-1})		
BIAP (Fig. 2A)	apo BIAP (Fig. 2B)	Tentative assignments
1682		νC=O amide I (β-sheet)[45]
1660		νC=O amide I (turn)[45]
1651–1652	1652	νC=O amide I (α-helix)[45]
1633	1633	νC=O amide I (β-sheet)[45]
1586–1577	1586–1571	νC=O COO^- Asp or Glu[46]
1547	1547	δN-H amide II[45]
1516–1517	1516–1517	ν ring OH Tyr[46]
1443	1455	δ N-^{2}H amide II′ and ^{2}HOH[45]

Influence of Temperature on ANS Fluorescence in the Presence of Native Alkaline Phosphatase and Apoenzyme

It is well known that ANS fluorescence quantum yield increases upon binding noncovalently to hydrophobic proteins regions. Therefore, it was used to monitor the thermal denaturation of native and metal-depleted BIAP (Fig. 8). At 20°C, BIAP, in its native conformation, exhibited few hydrophobic regions accessible to ANS. At this non-denaturing temperature, metal-depleted enzyme exposed more hydrophobic regions than BIAP because the ANS fluorescence intensity in the presence of apoBIAP was the highest. Temperature increase modified the intensity of the ANS fluorescence at 490 nm, which reached a maximum at 75°C for both proteins. Moreover, this effect was more important for BIAP (with an increase of about 12 times) than for apoBIAP (with an increase of 2 times). These results indicate that the exposure of hydrophobic regions was more progressive but less important with apoBIAP than with BIAP. This effect may be related to the loss of tertiary structure in the absence of divalent ions.

DISCUSSION

It is well known that the elimination of divalent ions from metalloenzymes could induce different conformational changes and/or the loss of enzymatic activity.[49,50] Here we studied the influence of divalent ions on the enzymatically active structure of alkaline phosphatase from bovine intestinal mucosa. Consequently, apoBIAP was prepared using ion-chelating agents. The metal-depleted enzyme exhibited a dramatic decrease of its phosphatase activity as compared to the native enzyme. Addition of metal ions (Zn^{2+} and/or Mg^{2+}) to apoBIAP did not induce significant reactivation.

We analyzed the quaternary structure modifications of BIAP following ion depletion by rate-zonal centrifugation and electrophoresis. We demonstrated that the loss of divalent ions leads to monomerization process. This did not agree with previous work on ECAP, where no monomerization process was detected in the presence of chelating agents.[51] Thus our results are the first evidence of a monomerization process for metal-depleted AP and show that the behavior of BIAP and ECAP is different. On the

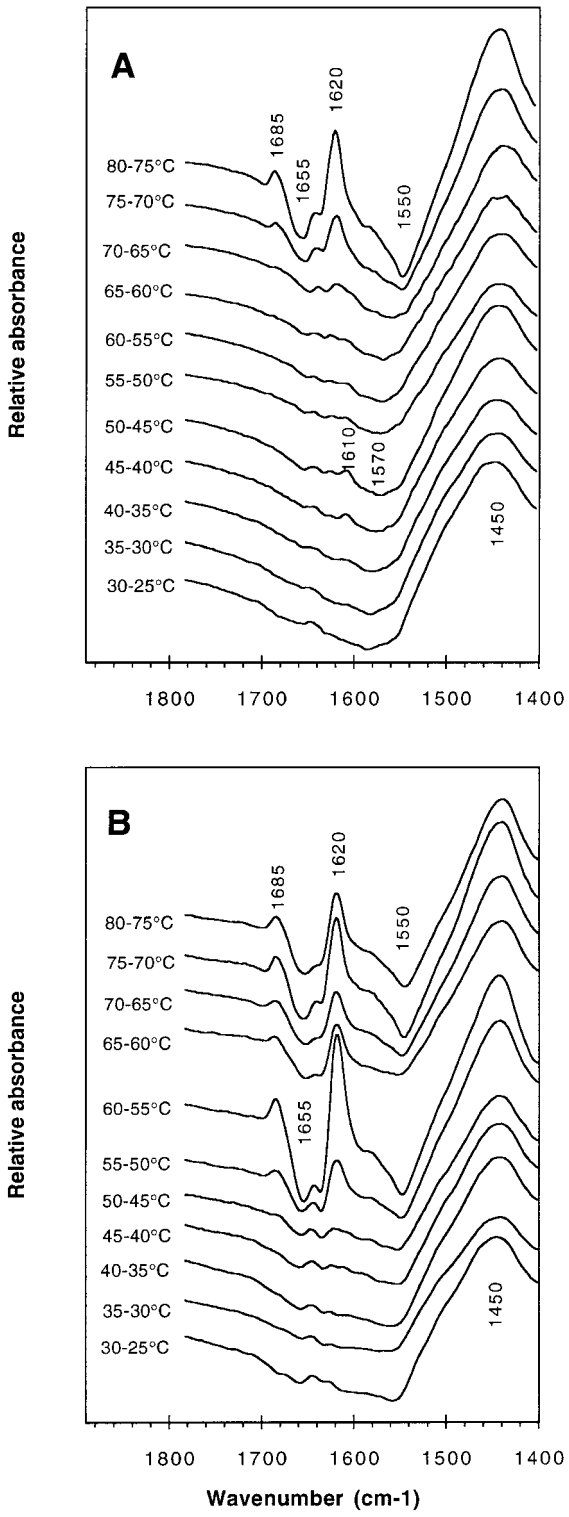

Fig. 5. Influence of temperature on the FTIR difference spectra of alkaline phosphatase in ^2H_2O (10 mg/ml). **(A)**: BIAP difference spectra. **(B)**: apoBIAP difference spectra. Each IR difference spectrum was calculated by subtracting the FTIR spectra recorded at two different temperatures at 5°C intervals as indicated on the figure.

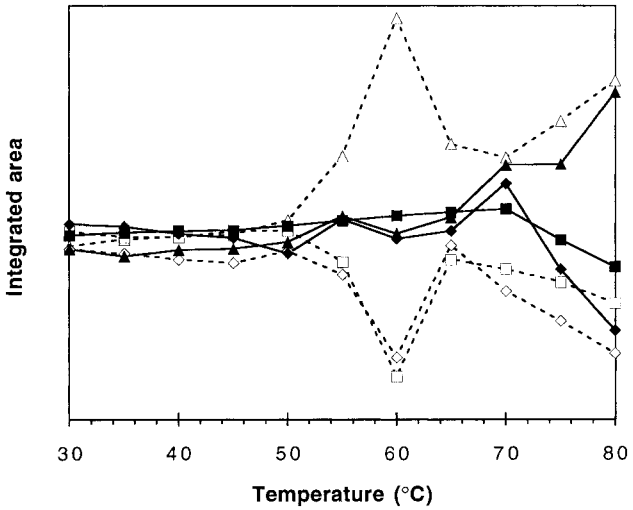

Fig. 6. Comparaison of the effect of temperature on some secondary structures and on N-H deuteration. BIAP (full symbols) and apoBIAP (open symbols). Appearance of β-sheets (triangles), disappearance of α-helices (squares) and H/^{2}H exchange (losange) were measured as the integrated area of the band centered at 1620, 1655 and 1550 cm^{-1}, respectively, in the IR difference spectra of Figure 5.

opposite of ECAP, the structure of BIAP has not been determined and the possibility that the metal binding sites are located at the monomer interface cannot be ruled out. Such a metal-dependency of oligomeric structure retaining has been reported for other metalloproteins. Removal of zinc ions from aspartate transcarbamoylase (an allosteric zinc-enzyme) induced dissociation into regulatory dimers and catalytic trimers.[52] Exposure of yeast alcohol dehydrogenase to chelating agents allowed the dissociation into four equal subunits.[53] Staphylococcal enterotoxin revealed two bound Zn^{2+} coordinated by residues from both subunits in the dimer interface, thus contributing directly to the formation of dimer.[54] For the cyanobacterial repressor SmtB, which binds two Zn^{2+} per subunit, stronger dimerization was observed upon metal-binding.[55]

Studies of ANS binding on BIAP showed that there were more regions accessible for ANS in apoenzyme than in native enzyme. These regions might be generated by the dissociation of dimer to monomer or by size increase of the protein.

Divalent ions are not only necessary for the stabilization of the quaternary structure of BIAP but they are also involved in the secondary and tertiary structures of the protein. The elimination of divalent ions from BIAP was probed by using FTIR spectroscopy (as shown by the decrease of the COO^- band at 1,595–1,577 cm^{-1} in the apoBIAP). This removal induced conformational changes as proved by intrinsic fluorescence determinations, indicating that some Trp residues were more accessible to the solvent molecules in the ion-depleted enzyme than in the native enzyme. These changes might correspond (i) to the disappearance of α-helices and/or turns with a concomitant appearance of unordered structures and β-sheets and (ii) to the more ANS-accessible regions of apoBIAP. These

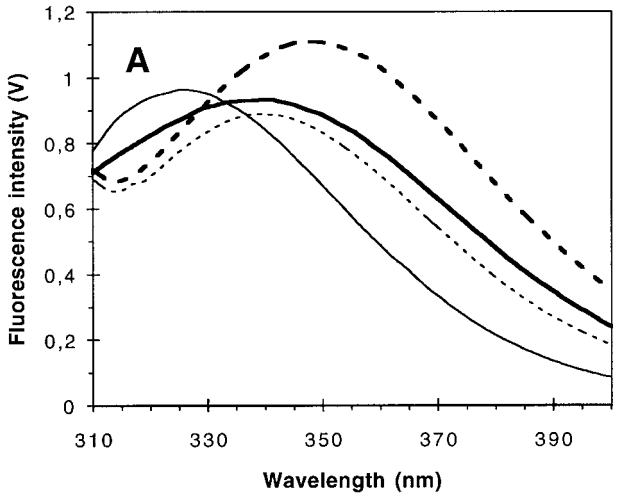

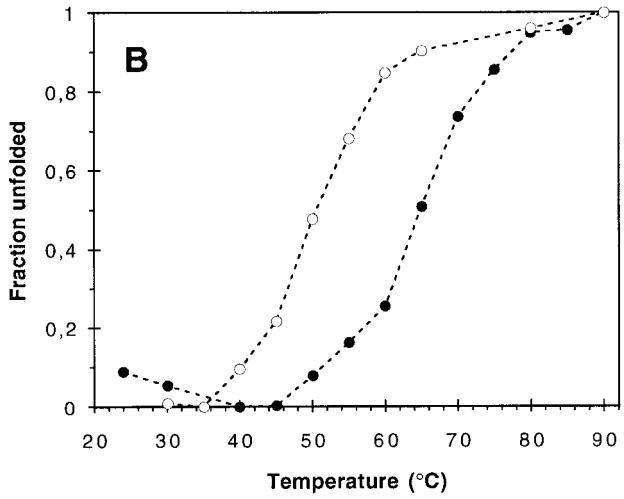

Fig. 7. Effect of temperature on the fluorescence emission of alkaline phosphatase (100 µg/mL). **(A)** BIAP (—), heat-denatured BIAP (---), apoBIAP (—) and heat-denatured apoBIAP (---) fluorescence spectra were recorded at 25°C (without heating) and 85°C (for heat-denatured forms). **(B)**: Thermal unfolding transition of BIAP (●) and apoBIAP (○) in metal-free 20 mM Tris-HCl pH 7.5 buffer, determined from the intensity-weighted average emission wavelength ⟨λ⟩. Excitation wavelength was 290 nm.

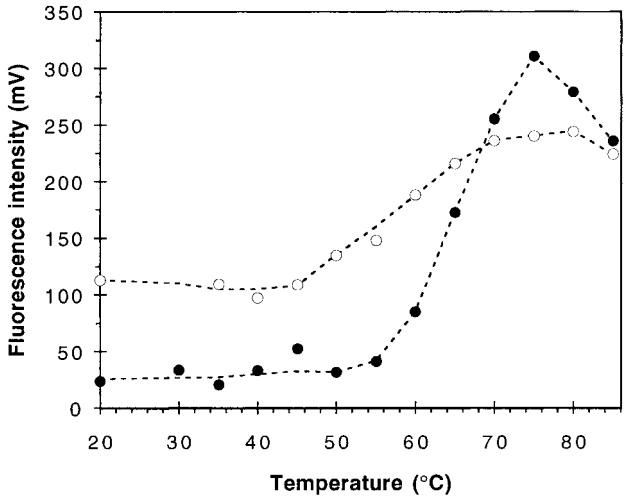

Fig. 8. Temperature dependency of ANS fluorescence in the presence of alkaline phosphatase. ANS (19 µM) was incubated with 200 µg/mL BIAP (●) or apoBIAP (○) in metal-free 20 mM pH 7.5 Tris-HCl buffer. Excitation wavelength was 380 nm and fluorescence was recorded at 490 nm.

conformational changes did not correspond to the complete unfolding of the protein. Indeed, the ANS fluorescence intensity and the shift of Trp fluorescence emission maximum reached their maximum values after thermal denaturation. In the same way, the most important changes in apoBIAP FTIR spectra were obtained by raising temperature. All the metal depletion-induced modifications in the secondary and tertiary structures of the BIAP subunits could generate the formation of a dimer with a very low specific activity and finally allow to inactive monomers. Furthermore this apoBIAP monomer seems to be different of that obtained by incubation of BIAP at 100°C in the presence of SDS 2% because it runs differently in the sucrose gradient. Thus the apoBIAP monomer is partially unfolded.

Concerning the influence of temperature on the conformation of BIAP, three steps were exhibited. The first one, corresponding to the loss of BIAP activity (at 45–60°C), was correlated to modifications of the enzyme conformation. Indeed, this temperature range induced some minor changes in the FTIR spectra (at 40–50°C). These FTIR changes could correspond to modifications of strength of the ion-binding with Asp and/or Glu COO^- groups and to the deuteration of Arg residues near the metal binding sites. Such an explanation agrees with a previous study on the primary sequence of the active site of BIAP, demonstrating the presence of Arg, Asp, and Glu residues.[36] The second temperature-induced step, appearing at about 60°C, corresponds to the thermal unfolding transition of BIAP probed by intrinsic fluorescence (at 65°C) and the appearance of hydrophobic regions becoming accessible to ANS. This second step might correspond to the heat-induced monomerization. Such a monomerization was described previously for ECAP.[51] The third step, after 70°C, might reflect the temperature-induced aggregation of BIAP and corresponds to the formation of intermolecular β-sheets with a concomittant loss of some α-helices (as determined by FTIR spectroscopy).

When the enzyme was ion-depleted, only one step of temperature-induced conformational changes was exhibited. Indeed, the loss of the residual activity of apoBIAP corresponds to the conformational changes (first appearance of intermolecular β-sheets and thermal unfolding transition) observed at 55–60°C. Such intermolecular β-sheets were in accordance with the aggregation of thermally denatured apoBIAP observed by a centrifugation analysis. This difference between BIAP and apoBIAP in the behavior towards temperature agrees with the results

of Chlebowski and Mabrey on ECAP.[56] Calorimetric investigations of the apoECAP dimer demonstrated that the progressive increase in the thermodynamic stability of the enzyme was associated with the occupation of the Zn^{2+} binding sites.

After addition of metal ions to apoBIAP no appreciable recovery of enzymatic activity was obtained. This indicated that either (i) the metal depletion of BIAP leads to such important modifications in secondary and tertiary structures of the subunits that the ion addition could not induce dimer formation or (ii) the dimer was formed with wrong rearrangements, shielding some native metal-binding amino acids and/or discover other metal-binding residues. The so-formed dimer was catalytically less active.

In the case of ECAP monomers (obtained by heat and pH denaturation), reactivation was possible but involved the dimerization process in which Zn^{2+} ions were essential.[51,57] The proposed pathway of ECAP renaturation consists of the subunit refolding to form a Zn^{2+} binding site and then binding of Zn^{2+} followed by dimerization.[57] It should be noticed that this Zn^{2+} dependency may not represent an absolute requirement for dimerization because *E. coli* grown in the absence of Zn^{2+} synthethize a dimeric apoECAP.[58]

In conclusion, our work on the role of metal ions on secondary and quaternary structure of BIAP proved two main differences compared to ECAP. The loss of the divalent ions from the enzyme induces monomerization of the protein and the restoration of the enzyme activity by adding divalent ions (Zn^{2+} and/or Mg^{2+}) has been impossible under our used conditions. The research of conditions for more complete reactivation of the enzyme and the induced conformational changes is in progress.

ACKNOWLEDGMENTS

We are grateful to B. Couturier for his helpful discussions concerning protein unfolding. We would also like to thank Pr. P. Coulet for providing us access to Nicolet 510 M FTIR spectrometer and E. Seinturier for her technical assistance.

REFERENCES

1. Coleman JE, Gettins P. Alkaline phosphatase, solution structure and mechanism. Adv Enzymol Relat Areas Mol Biol 1983;55:381–452.
2. Coleman JE. Structure and mechanism of alkaline phosphatase. Annu Rev Biophys Biomol Struct 1992;21:441–483.
3. Ghosh SS, Bock SC, Rokita SE, Kaiser ET. Modification of the active site of alkaline phosphatase by site directed mutagenesis. Science 1986;231:145–148.
4. Butler-Ransohoff JE, Kendall DA, Kaiser ET. Use of site-directed mutagenesis to elucidate the role of Arg 166 in the catalytic mechanism of alkaline phosphatase. Proc Natl Acad Sci USA 1988;85:4276–4278.
5. Chaidaroglou A, Brezinski DJ, Middleton SA, Kantrowitz ER. Function of Arg 166 in the active site of *Escherichia coli* alkaline phosphatase. Biochemistry 1988;27:8338–8343.
6. Chaidaroglou A, Kantrowitz ER. Alteration of Asp 101 in the active site of *Escherichia coli* alkaline phosphatase enhances the catalytic activity. Protein Eng 1989;3:127–132.
7. Mandecki W, Shallcross MA, Sowadski J, Tomazic-Allen S. Mutagenesis of conserved residues within the active site of *Escherichia coli* alkaline phosphatase yields enzymes with increased kcat. Protein Eng 1991;4:801–804.
8. Butler-Ransohoff JE, Rokita SE, Kendall DA, Banzon JA, Carano KS, Kaiser ET, Matlin AR. Active-site mutagenesis of *Escherichia coli* alkaline phosphatase: replacement of serine-102 with nonnucleophilic amino acids. J Org Chem 1992;57:142–145.
9. Xu X, Kantrowitz ER. The importance of aspartate 327 for catalysis and zinc binding in *Escherichia coli* alkaline phosphatase. J Biol Chem 1992;267:16244–16251.
10. Xu X, Kantrowitz ER. Binding of magnesium in a mutant *Escherichia coli* alkaline phosphatase changes the rate-determining step in the reaction mechanism. Biochemistry 1993;32:10683–10691.
11. Ma L, Kantrowitz ER. Mutations at histidine 412 alter zinc binding and eliminate transferase activity in *Escherichia coli* alkaline phosphatase. J Biol Chem 1994;269:31614–31619.
12. Xu X, Qin XQ, Kantrowitz ER. Probing the role of histidine-372 in zinc binding and the catalytic mechanism of *Escherichia coli* alkaline phosphatase by site-specific mutagenesis. Biochemistry 1994;33:2279–2284.
13. Sowadski JM, Handschumacher MD, Murthy HMK, Foster BA, Wickoff HW. Refined structure of alkaline phosphatase from *Escherichia coli* at 2.8 Å resolution. J Mol Biol 1985;186: 417–433.
14. Kim EE, Wyckoff HW. Reaction mechanism of alkaline phosphatase based on crystal structures. J Mol Biol 1991;218:449–464.
15. Chen L, Neidhart D, Kohlbrenner WM, Mandecki W, Sowadski J, Abad-Zapatero C. 3-D structure of a mutant (Asp101→Ser) of *Escherichia coli* alkaline phosphatase with higher catalytic activity. Protein Eng 1992;5:305–310.
16. Chaidaroglou A, Kantrowitz ER. The Ala-161→Thr substitution in *Escherichia coli* alkaline phosphatase does not result in loss of enzymatic activity although the homologous mutation in humans causes hypophosphatasia. Biochem Biophys Res Commun 1993; 193:1104–1109.
17. Murphy JE, Xu X, Kantrowitz ER. Conversion of a magnesium binding site into a zinc binding site by a single amino acid substitution in *Escherichia coli* alkaline phosphatase. J Biol Chem 1993;268:21497–21500.
18. Tibbitts TT, Xu X, Kantrowitz ER. Kinetics and crystal structure of a mutant *Escherichia coli* alkaline phosphatase (Asp-369→Asn): a mechanism involving one zinc per active site. Protein Sci 1994;3:2005–2014.
19. Dealwis CG, Brennan C, Christianson K, Mandecki W, Abadzapatero C. Crystallographic analysis of reversible metal binding observed in a mutant (Asp153→Gly) of *Escherichia coli* alkaline phosphatase. Biochemistry 1995;34:13967–13973.
20. Dealwis CG, Chen LQ, Brennan C, Mandecki W, Abadzapatero C. 3-D structure of the D153G mutant of *Escherichia coli* alkaline phosphatase: an enzyme with weaker magnesium binding and increased catalytic activity. Protein Eng 1995;8:865–871.
21. Ma L, Tibbitts TT, Kantrowitz ER. *Escherichia coli* alkaline phosphatase: X-ray structural studies of a mutant enzyme (His-412→Asn) at one of the catalytically important zinc binding sites. Protein Sci 1995;4:1498–1506.
22. Ma L, Kantrowitz ER. Kinetic and X-ray structural studies of a mutant *Escherichia coli* alkaline phosphatase (His-412→Gln) at one of the zinc binding sites. Biochemistry 1996;35:2394–2402.
23. Tibbitts TT, Murphy JE, Kantrowitz ER. Kinetic and structural consequences of replacing the aspartate bridge by asparagine in the catalytic metal triad of *Escherichia coli* alkaline phosphatase. J Mol Biol 1996;257:700–715.
24. Coleman JE. Multinuclear nuclear magnetic resonance approaches to the structure and mechanism of alkaline phosphatase. In: Torriani-Gorini A, Rothman FG, Silver S, Wright A, Yagil E, editors. Phosphate metabolism and cellular regulation in microorganisms. Washington, DC: American Society of Microbiology; 1987. p 127–138.
25. Simpson RT, Vallee BL, Tait GH. Alkaline phosphatase of *Escherichia coli*: composition. Biochemistry 1968;7:4336–4342.
26. Anderson R, Bosron W, Kennedy F, Vallee B. Role of magnesium in *Escherichia coli* alkaline phosphatase. Proc Natl Acad Sci USA 1975;72:2989–2993.
27. Harkness D. Studies on human placental alkaline phosphatase II. Kinetic properties and studies on the apoenzyme. Arch Biochem Biophys 1968;126:513–523.

28. Brunel C, Cathala G. Activation and inhibition processes of alkaline phosphatase from bovine brain by metal ions (Mg^{2+} and Zn^{2+}). Biochim Biophys Acta 1973;309:104–115.
29. Ey PL, Ferber E. Calf thymus alkaline phosphatase-I. Properties of the membrane-bound enzyme. Biochim Biophys Acta 1977;480: 403–416.
30. PetitClerc C, Fecteau C. Mechanism of action of Zn^{2+} and Mg^{2+} on rat placenta alkaline phosphatase. II. Studies on membrane-bound phosphatase in tissue sections and in whole placenta. Can J Biochem 1977;55:474–478.
31. Jahan M, Butterworth P. Alkaline phosphatase of chick kidney. Enzyme 1986;35:61–69.
32. Ciancaglini P, Pizauro J, Leone F. Polyoxyethylene 9-lauryl ether-solubilized alkaline phosphatase: synergistic stimulation by Zn and Mg ions. Int J Biochem 1992;24: 611–615.
33. Leone FA, Ciancaglini P, Pizauro JM, Rezende AA. Rat osseous plate alkaline phosphatase: mechanism of action of manganese ions. Biometals 1995;8:86–91.
34. Kim EE, Wyckoff HW. Structure of alkaline phosphatases. Clin Chim Acta 1989; 186:175–188.
35. Low MG. The glycosyl-phosphatidylinositol anchor of membrane proteins. Biochim Biophys Acta 1989;988:427–454.
36. Culp JS, Hermodson M, Butler LG. The active site and amino-terminal acid sequence of bovine intestinal alkaline phosphatase. Biochim Biophys Acta 1985;831:330–334.
37. de la Fourniere L, Nosjean O, Buchet R, Roux B. Thermal and pH stabilities of alkaline phosphatase from bovine intestinal mucosa: a FTIR study. Biochim Biophys Acta 1995;1248:186–192.
38. Holmquist B. Elimination of adventitious metals. Method Enzymol 1988;158:6–12.
39. Ryrie IJ, Gallagher A. The yeast mitochondrial ATPase complex: subunit composition and evidence for a latent protease contaminant. Biochim Biophys Acta 1979;545:1–14.
40. Laemmli UK. Cleavage of structural proteins during the assembly of the head of bacteriophage T4. Nature 1970;227:680–685.
41. Gross M, Lustig A, Wallimann T, Furter R. Multiple state equilibrium unfolding of guanidino kinases. Biochemistry 1995;34:10350–10357.
42. Bandekar J. Amides modes and protein conformations. Biochim Biophys Acta 1992;1120:123–143.
43. Susi H. Infrared spectroscopy-conformations. Methods Enzymol 1972;26:455–472.
44. Krimm S, Bandekar J. Vibrational spectroscopy and conformation of peptides, polypeptides and proteins. Adv Protein Chem 1986;38: 181–386.
45. Surewicz WK, Mantsch HH. Infrared absorption methods for examining protein structure. In: Havel HA, editor. Spectroscopic methods for determining protein structure in solution. United Kingdom: VCH Publishers; 1996. p 135–162.
46. Goormaghtigh E, Cabiaux V, Ruysschaert JM. Determination of soluble and membrane protein structure by Fourier transform infrared spectroscopy I. Assignments and model coumponds in subcellular biochemistry. In: Hilderson HJ, Ralston GB, editors. Physical methods for the study of biomembranes. Vol. 23. New York: Plenum Press; 1994. p 329–362.
47. Mizuguchi M, Nara M, Yue K, Kawano K, Hiaoki T, Nitta K. Fourier transform infrared spectroscopic studies on the coordination of the side chain COO^- groups to Ca^{2+} in equine lysozyme. Eur J Biochem 1997;250:72–76.
48. Mizuguchi M, Nara M, Kawano K, Nitta K. FT-IR study of the Ca^{2+}-binding to bovine α-lactalbumin. Relationships between the type of coordination and characteristics of the bands due to the Asp COO^- groups in the Ca^{2+}-binding site. FEBS Lett 1997;417: 153–156.
49. Voss T, Meyer R, Sommergruber W. Spectroscopic characterization of rhinoviral protease 2A: Zn is essential for the structural integrity. Protein Sci 1995;4:2526–2531.
50. Huang CC, Lesburg CA, Kiefer LL, Fierke CA, Christianson DW. Reversal of the hydrogen bond to zinc ligand histidine-119 dramatically diminishes catalysis and enhances metal equilibration kinetics in carbonic anhydrase II. Biochemistry 1996;35:3439–3446.
51. Schlesinger MJ, Barrett K. The reversible dissociation of alkaline phosphatase of *Escherichia coli*. I-Formation and reactivation of subunits. J Biol Chem 1965;240:4284–4292.
52. Nelbach ME, Pigiet VPJ, Gerhart JC, Schachman HQ. A role for zinc in the quaternary structure of aspartate transcarbamoylase from *Escherichia coli*. Biochemistry 1972;11:315–327.
53. Kägi JHR, Vallee BL. The role of zinc in alcohol dehydrogenase V. The effect of metal-binding agents on the structure of the yeast alcohol dehydrogenase molecule. J Biol Chem 1960;235:3188–3192.
54. Sundstrom M, Abrahmsen L, Antonsson P, Mehindate K, Mourad W, Dohlsten M. The crystal structure of staphylococcal enterotoxin type D reveals Zn^{2+}-mediated homodimerization. EMBO J 1996;15:6832–6840.
55. Kar SR, Adams AC, Lebowitz J, Taylor KB, Hall LM. The cyanobacterial repressor SmtB is predominantly a dimer and binds two Zn^{2+} ions per subunit. Biochemistry 1997;36:15343–15348.
56. Chlebowski JF, Mabrey S. Differential scanning calorimetry of apo-, apophosphoryl, and metalloalkaline phosphatases. J Biol Chem 1977;252:7042–7052.
57. McCracken S, Meighen EA. Evidence for histidyl residues at the Zn^{2+} binding sites of monomeric and dimeric forms of alkaline phosphatase. J Biol Chem 1981;256:3945–3950.
58. Harris M, Coleman JE. The biosynthesis of apo- and metalloalkaline phosphatases of *Escherichia coli*. J Biol Chem 1968;243:5063–5073.